Real Time Tracker Based Upon Local Hit Correlation Circuit for Silicon Strip Sensors

Niklaus Lehmann[a,*], Lorenzo Pirrami[b], Carl Haber[a], Sergio Diez[a,c], Haichen Wang[a], Nandor Dressnandt[d], Silvan Duner[b], Maurice Garcia-Sciveres[a], Amogh Halgeri[d], Paul Keener[d], John Keller[c], Mitchell Newcomer[d], Jacob Pasner[e], Richard Peschke[c], Amar Risbud[f], Eric Ropraz[b], Jonas Stalder[b]

[a] *Lawrence Berkeley National Laboratory, 1 Cyclotron Road, Berkeley, CA, 94720, USA*
[b] *University of Applied Sciences Western Switzerland, Boulevard de Pérolles 80 - CP 32, CH-1705 Fribourg, Switzerland*
[c] *Deutsches Elektronen-Synchrotron, Notkestraße 85, 22607 Hamburg, Germany*
[d] *University of Pennsylvania, Philadelphia, PA 19104, USA*
[e] *University of California Santa Cruz, 1156 High Street, Santa Cruz, CA 95064, USA*
[f] *University of California Berkeley, Berkeley, CA 94720, USA*

Abstract

ATLAS is a general purpose experiment at the Large Hadron Collider (LHC) at CERN. For the planned high luminosity upgrade of the LHC, a significant performance improvement of the ATLAS detector is required, including a new tracker and a new trigger system that makes use of charged track information early on. The current ATLAS baseline is to seed the lowest trigger level with calorimeter and muon information only, but exploration of real time track correlation as described in this note is nevertheless of interest, as the upgraded trigger design has not yet been finalized.

The latest prototype ATLAS strip detector readout chip (ABC130) includes a new readout scheme in parallel with conventional readout, called the Fast Cluster Finder (FCF). The FCF is capable of finding hits within 6 ns and transmitting the found hit information synchronously every 25 ns. Using the FCF together with an external correlation logic makes it possible to look for pairs of hits consistent with tracks from the interaction point above a transverse momentum threshold. The correlator finds coincidences between two closely spaced parallel sensors, a "doublet", and can generate a information used as input to a lowest level trigger decision.

The correlation logic was developed as part of a demonstrator and was successfully tested in an electron beam. The results of this test beam experiment proved the concept of the real time track vector processor with FCF.

Keywords: Trigger concepts and systems (hardware and software), HL-LHC, silicon strip tracker, high speed readout

*Corresponding author.
E-mail address: nlehmann@lbl.gov (Niklaus Lehmann).

1. Introduction

An upgrade for the Large Hadron Collider (LHC) is under development and planned to be finished for the mid 2020's to become the High Luminosity LHC (HL-LHC). This upgrade is performed in multiple phases. One of the experiments is the general purpose detector ATLAS. The ATLAS Phase-II upgrade is designed to match the requirements of the increased luminosity in the HL-LHC [1]. The instantaneous luminosity is assumed to increase up to $7 \times 10^{34} cm^{-2} s^{-1}$. This requires a performance improvement in the trigger and data acquisition system (DAQ) to guarantee the physics performance of the ATLAS detector during operation.

Currently, ATLAS uses a Level 1 (L1) trigger with 100 kHz average rate to read the full data from the entire detector front end electronics. The planned baseline for the Phase-II upgrade is to insert a 1 MHz Level 0 (L0) trigger to retrieve full or partial tracker information, and then incorporate this information in a L1 decision to read the full experiment, with an average L1 rate of up to 400 kHz.

An alternative to relying on a L0 trigger would be to retrieve reduced information from the tracker at the full 40 MHz bunch crossing rate, as is the case for the calorimeter and muon systems. The correlator scheme described in this note allows to reduce tracker data volume in-situ and in real time, in order to make readout possible without any trigger signals. Data reduction is needed because full triggerless readout of all tracker data from every collision is not considered technically feasible with low mass and low power. The correlator approach provides a data reduction factor of 20 to 40 [2], comparable to the baseline of reading data from just 1 out of 40 collisions with an externally supplied 1 MHz L0.

The Compact Muon Solenoid (CMS) experiment tracker design for Phase-II is based on the principle of layer doublet correlations to read reduced tracker information from every collision [3], but their correlation hardware development is different from that presented here.

The idea of the real time tracker is to use the information from two adjacent detector layers. Hit information of detected particles is directly analyzed in real time in-situ every 25 ns, corresponding to the time between two collisions. A dedicated correlation logic, called "correlator", is implemented on the module. A module is an assembly of silicon sensors and readout electronics. The correlator reconstructs track vectors across two layers and filters them by the transverse incident angle, using the cluster size and azimuthal offset between the clusters on the two layers. The incident angle is correlated with the transverse momentum for particles coming from the interaction point. Secondary particles from interactions in the detector material can have any angle-momentum correlation and constitute a background. A sketch of the real time tracker concept is shown in figure 1. See also reference [4][1].

[1] The term "self-seeded trigger" is used in the references instead of real time tracker.

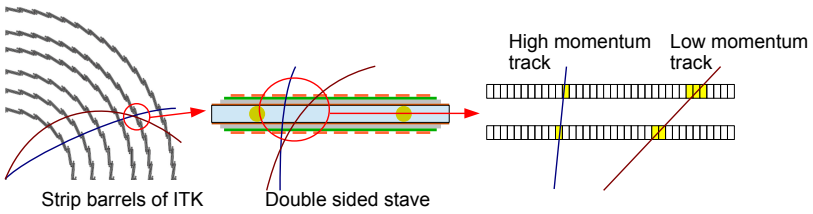

Figure 1: On the left is a sketch of the inner tracker strips barrel. The curvature of particle tracks depends on the momentum due to the applied magnetic field in the inner tracker. In the middle is a sketch of a stave cross-section with sensors on both sides. On the right is a drawing representing hits from two particles with incident angle on the two layers of strip sensors.

The baseline design of the Phase-II ATLAS strip tracker envisions silicon modules mounted on both faces of carbon composite actively cooled supports called staves. The stave core is made of a carbon fiber composite and is approximately 5mm thick [2]. The newest version of the front end application specific integrated circuit (ASIC) for reading the strip sensor is the Atlas Binary Chip 130 (ABC130). This chip includes a circuit called the Fast Cluster Finder (FCF), to find clusters within 6 ns and read out their digital positions once every 25 ns clock period. A cluster is defined here as one or two adjacent hit strips, because simulations showed that tracks of interest leave a cluster of the considered size [5]. 3 or more adjacent strips are ignored, as these are inconsistent with the small transverse incidence angles of interest. An exception are clusters that are broadened by delta rays, which we therefore will reject, incurring a $\sim$2% efficiency penalty.

The cluster information is serially transmitted at a speed of up to 640MHz. This fast readout provides the complete cluster information every 25 ns. An external correlator ASIC processes the cluster information to find coincidences. The correlator filters the coincidences depending on the incident angle. Only hits passing the filter are sent off-detector for use by the trigger system, without any level 0 trigger stage. Reference [6] discusses the FCF design while reference [7] describes the electronics for the ATLAS Phase-II upgrade.

In this work a proof of principle prototype correlator was developed with an FPGA [8]. The system contains four different printed circuit boards (PCBs): 1. FPGA board, 2. interface board (IB), 3. support board and 4. hybrid board , which are described in section 4. The correlator can read the FCF lines from two hybrid boards with 10 ABC130 chips and find coincidences between two rows of 1280 strips each. A doublet with two sensor modules was constructed to demonstrate the principle. The development of the demonstrator for the real time tracker was presented in reference [9], and reference [10] describes the final design used in the test beam experiment.

2. ABC130 with Fast Cluster Finder

The ABC130 is the newest generation of the ATLAS binary chip. It implements the front end electronics (FEE) chain for the ATLAS silicon strip tracker in the Phase-II upgrade. The ABC130 can read 256 channels, which are arranged in two rows and implemented as two separate 128-channel blocks, one for each row. Each channel has an individual FEE chain with a one bit analog to digital converter (ADC). The threshold of the ADC can be set globally for the chip. It is further possible to adjust the threshold of each channel to compensate small differences between the channels. An additional mask register allows to mask bad channels right after the ADCs.

There are two FCF logic blocks integrated in the ABC130, each working on one row of 128 channels and independent of the conventional readout. The FCF finds clusters of one or two hits for the reason explained in section 1. The FCF starts searching for clusters from both ends of the row, i.e. channel 0 and 127. Scanning from the ends towards the center, the FCF selects the first cluster smaller than three strips. Each FCF finds at most two clusters. In case there are more than two clusters, those in the middle are lost. Figure 2 gives an example how the cluster finder works.

The hit occupancy for the ATLAS inner tracker (ITk) is defined as the number of hits per module and per event divided by the number of readout channels per module. Under pile-up 200 conditions, i.e. 200 proton-proton collisions per bunch crossing, an occupancy of less than 1% is predicted. The end-cap regions of the detector exhibit the highest occupancy with ∼0.9% in the worst case [11]. Each ABC130 has 256 readout channels. Under the assumption of an even distribution of hits in each module, a 1% occupancy results in 2.6 hits per chip. As mentioned above, each ABC130 hosts two FCF lines, capable to detect two hits. Hence, it is possible to detect up to four hits per chip with the two FCF lines and therefore cover the maximum expected hit occupancy of the ITk. See also reference [1, 11] for more details of the expected hit occupancy.

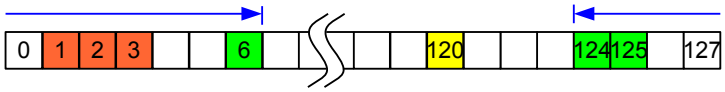

Figure 2: Sketch of the FCF search procedure for one bank, where each ABC130 has two of these blocks. Each square represents a strip and all the filled squares indicate a detected hit. The number in the squares is the strip address used by the ABC130. Strips 1 to 3 form a 3-hit cluster, which is ignored. A 2-hit cluster is observed at address 124 to 125 and a 1-hit cluster at address 6. These hits are valid and detected by the FCF. The hit at address 120 is also a valid 1-hit cluster but is ignored, because already two other clusters were found. The arrows indicate the direction of the cluster search.

The found clusters are transmitted serially on dedicated differential outputs. A dedicated fast clock (FCLK) is provided for the FCF readout. The two clusters found by each FCF are encoded with 16 bits, therefore an FCLK 16 times faster than beam crossing (BC) clock is required. The ABC130 was designed to work with an FCLK of up to 640 MHz for a 40 MHz BC.

References [6, 7, 12] give a more detailed description of the FCF and the ABC130 in general.

3. Correlation logic

The correlator would need to be realized in a dedicated radiation hard ASIC in an actual use case. In this work the correlator was implemented in a Virtex 6 FPGA to demonstrate the principle. The implemented correlator can read a double sided module (doublet) with 10 ABC130's on each side. This allows it to match the data from two rows of 1280 strips each. More details about the doublet are given in the next section.

The correlator is designed with multiple stages as shown in Figure 3. The first stage finds coincidences on the same row of both sensors. The second stage looks for coincidences across the different rows of strips on the two sensors, using the result from the first stage. The third stage transmits the found coincidences off the correlator chip. A detailed description of the correlator design and realization are given in references [8] and [10] respectively. A dedicated test and DAQ on a computer was used to acquire the found correlations for the studies shown here. See reference [10] for more details about the DAQ used.

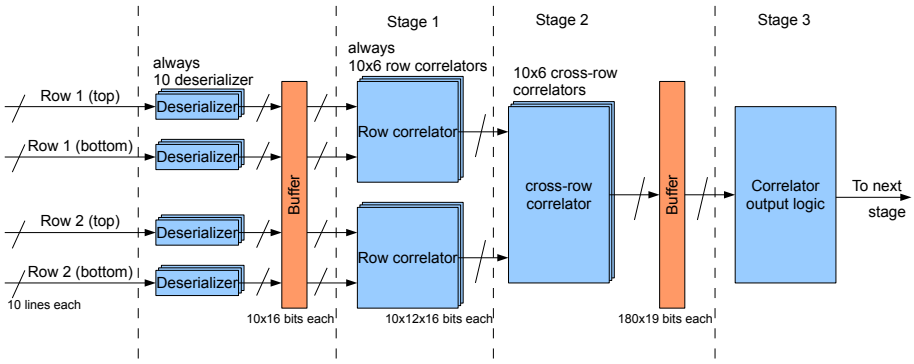

Figure 3: Correlator block diagram, reference [10]

The correlation logic is a purely combinatorial bloc that calculates the distance between all clusters found on the bottom and top layer of the doublet. The correlator considers only coincidences within a given range of offsets. A maximal distance of ± 3 strips is used for the measurements presented here. With the limited window size only a cluster from each chip pair plus the adjacent chips have to be compared. Some examples of possible correlation patterns are given in Figure 4.

4. Demonstrator setup

A physical demonstrator was built to test the real time tracker with FCF and correlator. The concept of the demonstrator is described in reference [9].

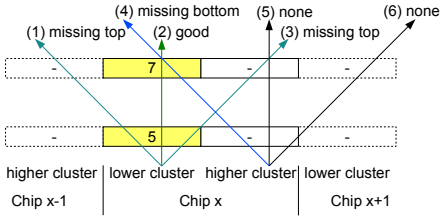

(a) Normal correlation

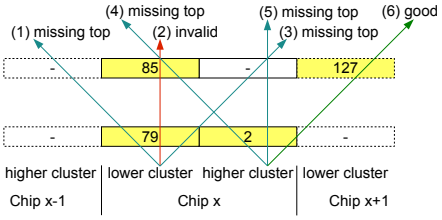

(b) Cross chip correlation and invalid correlation (out of window)

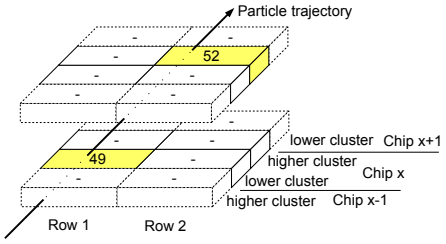

(c) Cross row correlation

Figure 4: Examples of different correlations. Each rectangle represents a cluster from the FCF. The numbers in the rectangles are the found addresses. The numbered arrows indicate the verified combination of bottom and top hits.

The electronics for the demonstrator are assembled on four PCBs:

- an FPGA board, which implements the correlations logic,
- an interface board (IB) provides drivers for the differential lines,
- a support board to hold the sensor and make the connectivity to the hybrid board,
- a hybrid board supporting the ABC130's together with the connection lines to the support board.

4.1. Electronic system

The ML605 development board [13] with a Xilinx Virtex 6 FPGA was used to implement the correlator. Several additional PCBs were developed to provide the connectivity and signal integrity from the FPGA to the ABC130's. A simplified block schematic is shown in Figure 5. The two support boards were mounted back to back to form the doublet. For each support board (top or bottom) exists a set of differential lines. The lines to the bottom board pass through the top board.

The communication between the FPGA and the ABC130 goes through differential lines. On the FPGA side the signals have the levels of the low voltage

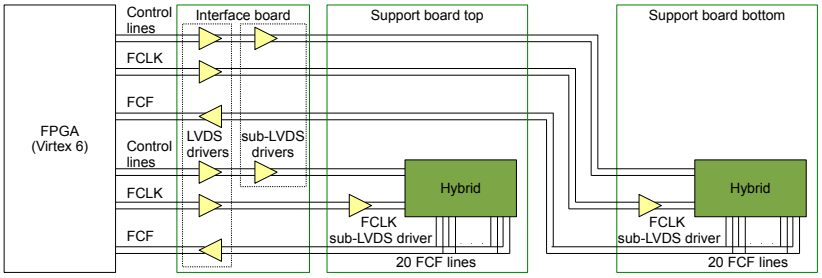

Figure 5: Simplified block schematic of the complete demonstrator. The control lines are BC, the readout clock (RCLK) and the command and trigger lines.

differential signaling (LVDS) standard. Because the ABC130 operates at a lower voltage, it uses a adjusted version of the LVDS with a smaller common voltage levels, called sub-LVDS.

The IB serves to adjust the levels on the differential lines from LVDS to sub-LVDS and is described in reference [14]. A transceiver chip designed by the Bonn ATLAS group was used to convert the LVDS signals from the FPGA [15]. This driver operates only up to a frequency of 320MHz. Therefore it was not possible to run the test at the goal design speed. Instead all the frequencies were divided by two, resulting in a 20MHz BC and 320MHz FCLK.

A support board provides the connectivity from the IB to the hybrid and serves also together with an aluminum plate as mechanical support for the sensor. The support board holds an sub-LVDS transceiver for the FCLK and provides the connectivity for the ABC130 power and sensor high voltage bias (HV) supplies. The FCLK is the most critical high speed signal going into the board and the corresponding transceiver was placed close to the hybrid to provide a better signal.

The ABC130's are mounted on a hybrid board, which is an PCB holding bare die and surface mount components. The hybrid includes the command and clock lines to the ABC130's together with the FCF output lines. A more detailed description is given in reference [16]. The hybrid used implements a "star" readout system with the FCF. This means that every chip is connected directly to a central node, which is here the correlator. As mentioned, the ABC130 has two FCF lines, each serving 128 of the 256 channels. All 10 chips per hybrid can be read in parallel with 20 differential lines. The layout of the hybrid with the FCF readout is shown in Figure 6. The central point for the connection to the correlator is on the left side of the board.

The boards are shown in Figure 7. There is a second module, consisting of support board, sensor and hybrid not visible in the picture, because it is mounted back to back to the first module. The sensor used is an ATLAS07 silicon strip sensor [17]. This sensor has four rows of strips, each 2.5cm long. There are two axial and two stereo rows. For the correlator only the axial rows are used.

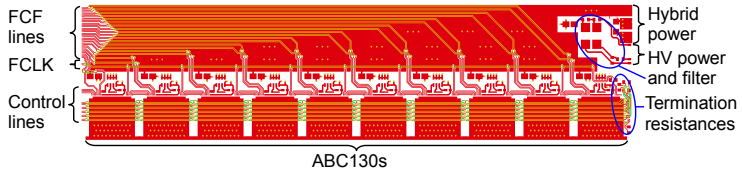

Figure 6: Layout of the hybrid with top and internal layer. The FCF lines are embedded in planes (not shown) to create a well shielded controlled impedance structure. The control lines are the clock, command and trigger lines for the ABC130's.

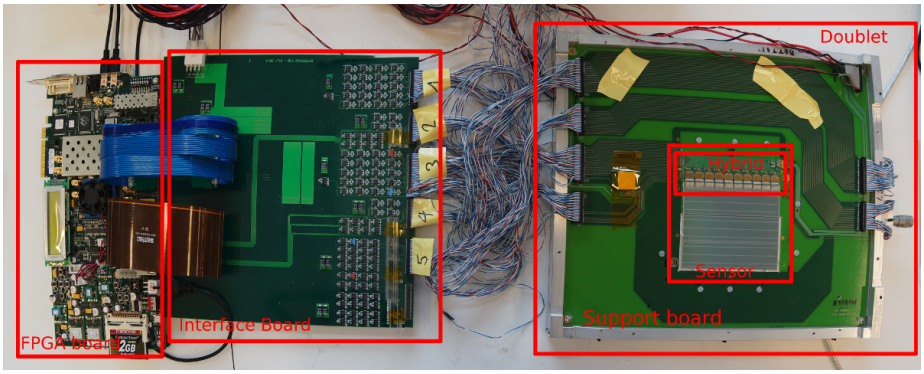

Figure 7: Picture of the complete demonstrator setup. On the left is the ML605 Virtex 6 development board. The middle PCB is the interface board. On the right is the doublet with one side visible. The sensor with the mounted hybrid is in the middle of the support board.

4.2. Doublet

The doublet was built to provide a test setup for the correlator. An aluminum frame provides the mechanical support. The support board is mounted on an insulated anodized aluminum plate and the area for the silicon sensor is cut out from the support board. A conductive HV frame held on the anodized plate holds the silicon sensor and creates the contact from the backplane to the HV contact on the support board. A closeup of the unfinished doublet is shown in Figure 8a. The sensor was glued with conductive epoxy to the HV frame. A screw makes electrical contact to the support board.

Figure 9 shows a schematic view of the doublet. To simulate a magnetic field in the test beam, one side of the doublet can be moved horizontally with a micrometer. The micrometer pushes the mobile side and two springs are used to create a counter force that pulls the mobile side back, in case of releasing the micrometer. This allowed the manual setting of an offset between the two sides. The springs and micrometer are shown in Figure 8b.

5. Test beam experiment

A test beam experiment was performed at the Stanford Linear Accelerator Center (SLAC). The correlator demonstrator was tested in a electron test beam

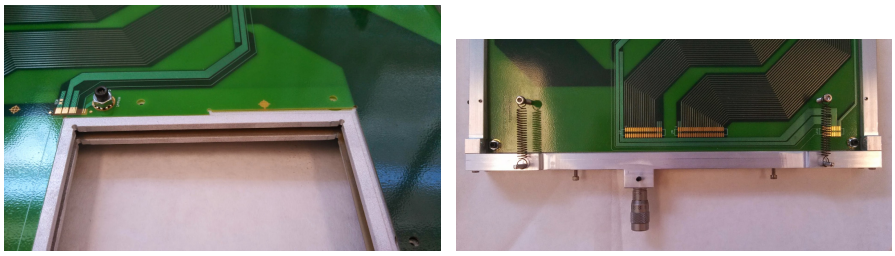

(a) Close up picture of the HV frame as a support and contact for the sensor bias voltage.

(b) Springs mounted on support board and frame. Micrometer to set the position in the middle of the picture.

Figure 8: Detail pictures of the unfinished doublet frame

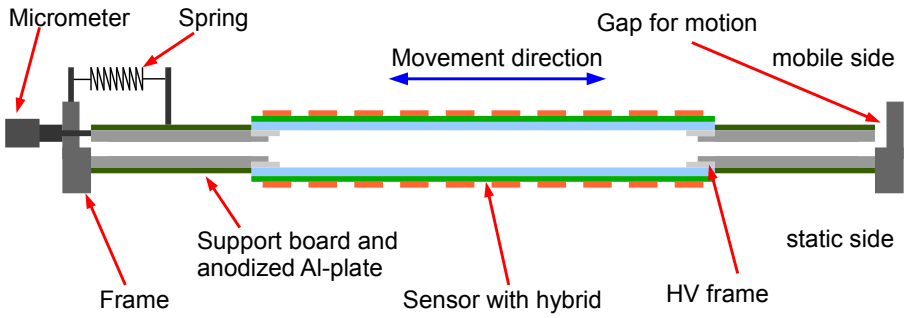

Figure 9: Sketch of the demonstrator doublet. View is a cut in the middle of the sensor, Reference [10, Fig. 5.15]

located at end station A (ESA) [18]. The EUDET telescope was used as a reference measurement [19]. The demonstrator is located in the middle of the telescope as can be seen in the setup shown in Figure 10.

The electron energy of the beam was in the range of 9-10 GeV with about 20 electrons per bunch. The beam frequency was 5Hz. Some variations were observed in intensity and energy because of changes from an experiment using the Linac Coherent Light Source (LCLS) at the same time. The EUDET telescope includes also a trigger logic unit (TLU) which generates a trigger signal together with an identifier for each event. The TLU makes its trigger decision based on two scintillators at the front of the setup and a signal coming from the accelerator. Each trigger is sent with an ID to all devices under test and helps to match offline the tracks from the telescope with the correlation found.

The doublet has a mobile side which can be moved with a micrometer as described in section 4.2. Several runs were performed at different positions of the micrometer. Each run consisted of 3000 events, where one event corresponds to a trigger from the TLU. The mobile side was moved in total over a distance of 640µm corresponding to over 8 strips. The complete region of the correlator acceptance window was covered with this movement.

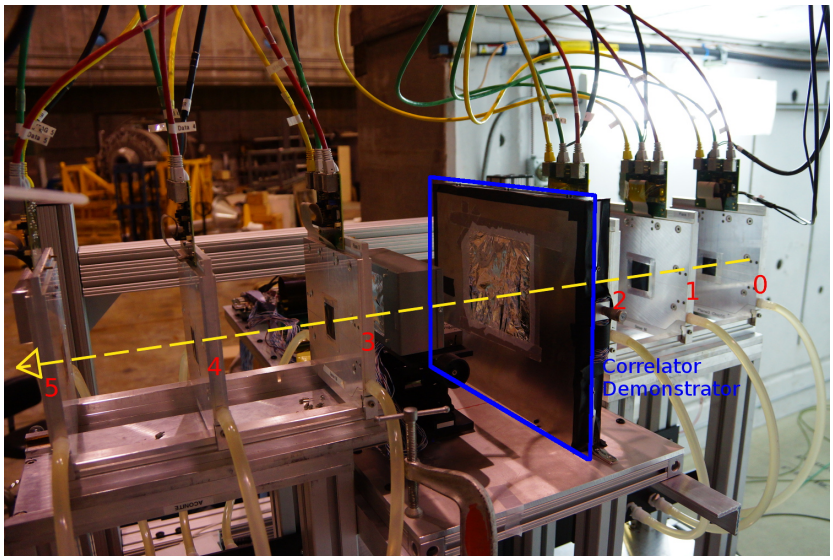

Figure 10: Test beam setup. The numbers indicate the layers of the EUDET telescope where layer 2 is hidden behind the demonstrator. The dashed arrow indicates the beam line.

6. Results

6.1. Beam profile

As a sanity check the distribution of the found correlations was plotted as a function of the correlation address to verify the beam profile. Figure 11 shows this result. It can be observed, that the beam was centered in the middle of the sensor. Row 2 saw a higher number of hits. Variations in the number of correlations are observed in the center part. The FCF sees only the two hits closest to the edge of a chip. Therefore the hits on the edge are favored and this results in peaks observed in the address plots. In practice, this is not a real problem because the instantaneous occupancy from the test beam was higher than the expected occupancy in the HL-LHC as described in section 2. Except for the peaks, which were identified as a result from the FCF, a similar beam profile was observed with the EUDET telescope.

6.2. Offset distribution

The beam passes through two collimators before arriving at the experiment setup. This limits the angular distribution of the the beam to a fraction of the angular resolution of the doublet. Therefore it is expected that the found correlations should have all the same offset. The offset from the correlations is plotted for two micrometer positions in Figure 12. A peak for a certain offset is observed together with background of correlations over all allowed offsets. The location of the peak depends on how the two sides are aligned, i.e. the micrometer position. Moving the mobile side with the micrometer results in a

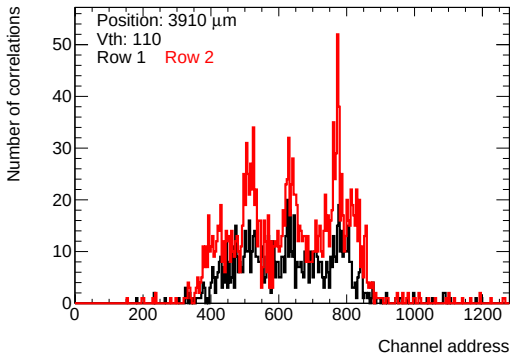

Figure 11: Address distribution for one micrometer position

displacement of the peak. A second offset value, right next to the peak observes also more correlations than the background and can be explained with an imperfect alignment of the two sides. It is supposed that the background contains spurious correlations. One possible source for these correlations is that they are coming from two hits close together. Other sources could be noise or scattering, where both should have a small contribution as discussed in reference [10]. The difference of 1 strip between the two rows comes from the wirebonding of the sensor as described in reference [10].

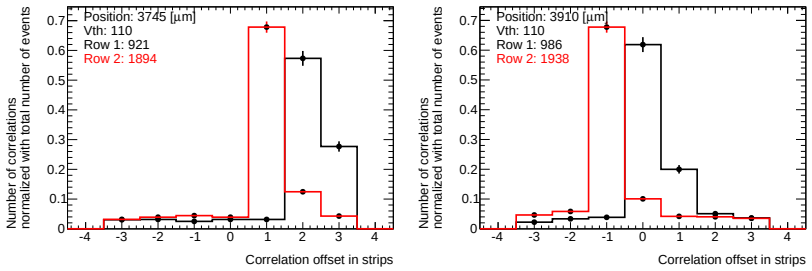

(a) (b)

Figure 12: Offset distribution plots for both rows. The total number of events is indicated for each row.

6.3. Filter and alignment with telescope tracks

The telescope information can be used to remove part of the spurious correlations from the data set. The found correlations were matched with the tracks reproduced from the EUDET telescope data for this purpose. The position of the reconstructed telescope tracks is calculated at the location of the correlator and the strip address is converted to the telescope coordinate system. The two

data sets were then matched to find tracks and correlations close together. In the y direction (up/down) a selection was performed on the telescope tracks to choose the correct strip row. In the x direction (left/right) a more accurate conversion was performed with the formula $x[mm] = 74.5\mu m \cdot x[strips] + \delta$. The $74.5\mu m$ correspond to the strip pitch, $x[strips]$ is the strip address on the static layer and δ is a conversion factor to match both sensors together. Using one fourth of the correlations found at each micrometer position, a δ of $44.95 \pm 0.03mm$ for row 1 and $44.88 \pm 0.03mm$ for row 2 was found. For this conversion we assume that the test beam is perpendicular to the silicon sensor.

The found conversion was applied to the rest of the data for a comparison with the EUDET telescope tracks. This allowed the elimination of some of the spurious correlations. Only a fraction of the observed correlation could be associated with telescope tracks, because the beam spot covered a larger area than the sensor area of the EUDET telescope. The pixel sensors used in the telescope have a surface of $2 \times 1cm^2$, which is much smaller than the active sensor area of $10 \times 5cm^2$ used by the correlator. Figure 13 shows the address distribution of the correlation matched with a telescope track, compared with all found correlations.

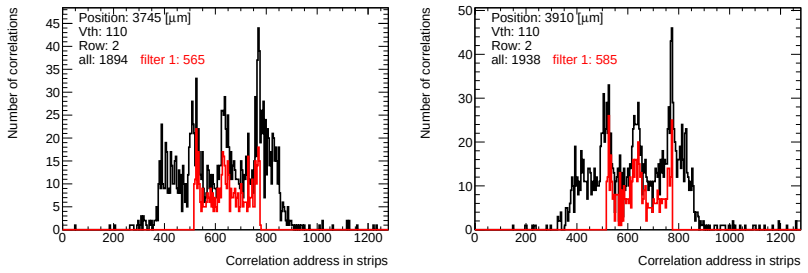

(a) (b)

Figure 13: Address distribution of all correlations and filtered correlations found. Filter 1 is all correlations with at least 1 track closer $0.08\mu m$.

The offset distribution of the filtered correlations is shown in Figure 14. There are two filters applied: Both filters select correlations with a track closer than $0.08\mu m$. Filter 2 has the additional restriction that only one track can be within $0.3\mu m$. The efficiency of the matching is not very high. Only $29 \pm 2.1\%$ of the correlations could be matched for filter 1 and $20 \pm 2.4\%$ for filter 2. Nevertheless the background could be reduced. The percentage of correlation located in the peak increased by $7 \pm 3\%$ for filter 1 and by $10 \pm 3\%$ for filter 2 compared to the result with no filter.

The further reduction of the background with selecting only correlations with only one nearby track supports the theory that spurious correlations are due to two electrons hitting two strips close together. Not all the spurious correlations forming the background could be removed though. Part of the remaining background could come from two hits close in x distance, but where

only one is detected by the EUDET telescope. This can happen because of the smaller telescope detector area.

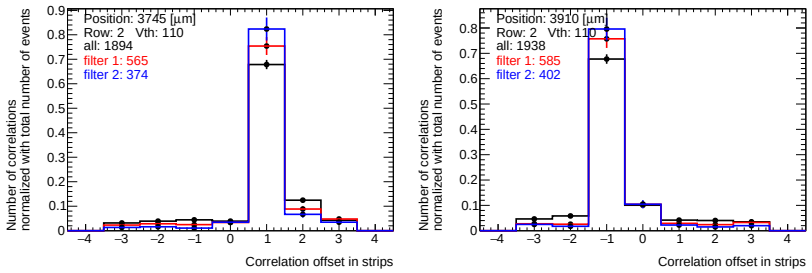

(a) (b)

Figure 14: Filtered distance distribution. Filter 1 is all correlations with at least 1 track closer $0.08\mu m$. Filter 2 is with only 1 track closer than $0.08\mu m$ and no other track closer than $0.3\mu m$.

Figure 15 shows the mean offset value as a function of the micrometer position. Only the matched correlations with filter 2 were used for these plots. A clear linear dependency can be observed as long as the offset is within the correlation window. Outside the window is a mean value close to 0. The two sides were not perfectly aligned, and the steps made not at an exact multiple of the strip pitch. This disturbs the mean, most visible at a position close to the edge of the window.

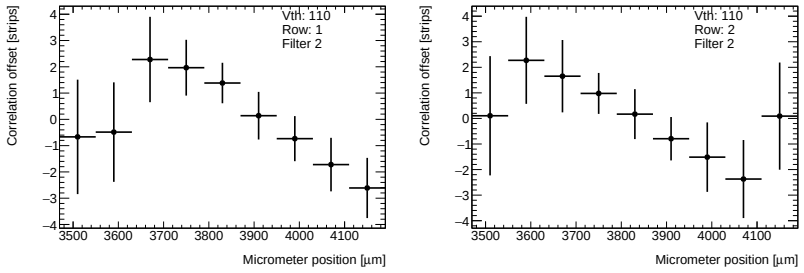

(a) (b)

Figure 15: Offset as function of micrometer position, using only matched correlations

7. Conclusion

The new Fast Cluster Finder feature in the ABC130 was used for the first time. Together with an FPGA system it was possible to build a correlator, that can detect coincidences between the two sides of a stave in real time. The

correlator logic and the doublet demonstrator are presented in this paper. The demonstrator can also be seen as a successful example of a star readout with fast (320MHz) transmission lines.

The demonstrator could be successfully operated in an electron test beam at SLAC to demonstrate the principle of the self-seeded trigger.

The next steps would be to improve further the correlation logic for a better rejection of spurious, wrong correlations. Another step would be to change the sub-LVDS drivers to support the full 640MHz on the FCF lines. Further work is in progress to build multiple doublets with the goal in building a telescope. Each doublet with a correlator would send the found correlations to a higher level "track correlator". This track correlator searches for coincidences between the different doublets to have an even better selection of valid tracks.

Acknowledgments

The authors would like to thank the personnel from SLAC who helped performing the test beam experiment.

The Bachelor and Master theses leading to the results of this paper were made possible thanks to an exchange program between the University of Applied Science Western Switzerland, the Ecole Polythéchnique Fédérale de Lausanne and the Lawrence Berkeley National Laboratory.

This work was supported by the Director, Office of Science, Offices of High Energy and Nuclear Physics of the U.S. Department of Energy under the Contracts DE-AC02-05CH11231.

References

[1] ATLAS Collaboration, "Letter of Intent for the Phase-II Upgrade of the ATLAS Experiment," Tech. Rep. CERN-LHCC-2012-022. LHCC-I-023, CERN, Geneva, Dec 2012.

[2] M. Garcia-Sciveres, M. Gilchriese, C. Haber, B. Heinemann, and T. Mueller, "System concepts for doublet tracking layers," *Journal of Instrumentation*, vol. 5, no. 10, p. C10001, 2010.

[3] L. Skinnari, "L1 track triggering at CMS for High Luminosity LHC," *Journal of Instrumentation*, vol. 9, no. 10, p. C10035, 2014.

[4] A. Schöning, "A self seeded first level track trigger for ATLAS," *Journal of Instrumentation*, vol. 7, no. 10, p. C10010, 2012.

[5] J. Arno, "Data Reduction At Front End Level in a Level-1 Track Trigger," July 2011. Diploma thesis in Physics for the Department of Physics and Astronomy at the University of Heidelberg.

[6] N. Dressanandt, A. Halgeri, M. Kamat, V. Koppal, and M. Newcomer, "Prompt trigger primitives for a self-seeded track trigger," *Journal of Instrumentation*, vol. 7, no. 10, p. C10001, 2012.

[7] T. Affolder, F. Anghinolfi, A. Clark, W. Dabrowskic, J. Dewitt, S. Diez Cornell, N. Dressdant, V. Fadeyev, P. Farthouat, D. Ferrere, A. Greenall, A. Grillo, J. Kaplon, M. Key-Charriere, D. La Marra, E. Lipeles, D. Lynn, M. Newcomer, F. Pereirab, P. Phillips, E. Spencer, K. Swientekc, M. Warren, and A. Weidberg, "System Electronics for the ATLAS Upgraded Strip Detector," Tech. Rep. ATL-UPGRADE-PUB-2013-011, CERN, Geneva, February 2013.

[8] L. Pirrami, "Fast triggering sensor module for the Large Hadron Collider," January 2014. Master Degree Thesis for University of Applied Sciences and Arts, Western Switzerland.

[9] S. D. Cornell, S. Duner, M. Garcia-Sciveres, C. Haber, N. Lehmann, L. Pirrami, E. Ropraz, and H. Wang, "Development of a Fast Cluster Finding self-seeded trigger demonstrator," *Journal of Instrumentation*, vol. 9, no. 12, p. C12022, 2014.

[10] N. Lehmann, "Tracking with self-seeded Trigger for High Luminosity LHC," August 2014. Master Degree Thesis for École Polytechnige Fédérale de Lausanne.

[11] S. Burdin, T. Cornelissen, C. Debenedetti, S. Elles, M. Elsing, I. Gavrilenko, N. Hessey, A. Huettmann, A. Korn, S. Miglioranzi, M. Lisovyi, P. Maettig, A. Schaelicke, A. Salzburger, K. Selbach, N. Styles, U. Soldevila, T. Todorov, J. Tseng, N. Valencic, P. Vankov, and P. Wells, "Tracking Performance of the Proposed Inner Tracker Layout for the ATLAS Phase-II Upgrade," Tech. Rep. ATL-UPGRADE-PUB-2013-001, CERN, Geneva, Feb 2013.

[12] ATLAS Collaboration, "ABC130 specification," 2013. 4.6Draft.

[13] XILINX, "ML605 Hardware User Guide UG534," October 2012. v1.8.

[14] S. Duner, "Trigger Functions for the High Luminosity LHC," August 2013. Bachelor Degree Thesis for University of Applied Sciences and Arts, Western Switzerland.

[15] M. Karagounis, "8 Channel LVDS Transceiver," December 2010. Version 1.0.

[16] E. Ropraz, "Sensor Module for the High Luminosity LHC," August 2013. Bachelor Degree Thesis for University of Applied Sciences and Arts, Western Switzerland.

[17] Y. Unno *et al.*, "Development of n-on-p silicon sensors for very high radiation environments," *Nuclear Instruments and Methods in Physics Research Section A: Accelerators, Spectrometers, Detectors and Associated Equipment*, vol. 636, no. 1, Supplement, pp. S24 – S30, 2011. 7th International.

[18] H. Fieguth, C. Hast, R. Iverson, J. Jaros, R. Jobe, *et al.*, "ESTB: A New Beam Test Facility at SLAC," *Conf.Proc.*, vol. C110328, pp. 1373–1375, 2011.

[19] EUDET Collaboration, "Detector Research and Development towards the International Linear Collider - Final Report," December 2010.